Opto-Electronic Advances

Supplementary information

September 2023, Vol. 6, No. 9

DOI: 10.29026/oea.2023.230012

Broadband and continuous wave pumped second-harmonic generation from microfiber coated with layered GaSe crystal

Zhen Hao, Biqiang Jiang*, Yuxin Ma, Ruixuan Yi, Xuetao Gan* and Jianlin Zhao

Key Laboratory of Light Field Manipulation and Information Acquisition, Ministry of Industry and Information Technology, and Shaanxi Key Laboratory of Optical Information Technology, School of Physical Science and Technology, Northwestern Polytechnical University, Xi'an 710129, China.

*Correspondence: BQ Jiang, E-mail: bqjiang@nwpu.edu.cn; XT Gan, E-mail: xuetaogan@nwpu.edu.cn

This file includes:

Supplementary information for this paper is available at https://doi.org/10.29026/oea.2023.230012

In this supplemental document we illustrate the fabrication method of the GaSe-transferred microfiber, the power dependence of third harmonic (TH) under picosecond pump, the broadband SH spectrum pumped by an amplified spontaneous emission (ASE) source, the origination of polarization dependent SH and calculation and calibration results of conversion efficiencies for references cited in Table 1.

Section 1: Chemical-free transfer method of the GaSe-transferred microfiber.

The GaSe-transferred microfiber was fabricated in 3 steps with a chemical-free transfer method, as shown in Fig. S1.

1. Multilayer GaSe crystalline was mechanically exfoliated from a bulk GaSe crystal with scotch tape.
2. Push the scotch tape onto a planar polydimethylsiloxane (PDMS), leaving the multilayered GaSe on the PDMS.
3. With the aid of a microscope, the PDMS with GaSe adhering on the surface is pressed down to the microfiber's tapered region. Remaining the pressing state for a few minutes until the GaSe is empirically determined to be transferred on the microfiber, then lift the PDMS upward. In this step, the ~30 mW red laser incident to the microfiber for ~20 minutes helps the layered GaSe to adhere onto the microfiber, when the PDMS was lifted away.

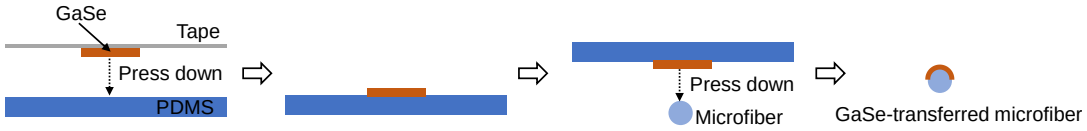

Fig. S1 | Fabrication process of the GaSe-transferred microfiber.

Section 2: Inherent distribution pattern of second harmonic and sum frequency peaks in the frequency region.

Circular frequencies of pump sources naturally satisfy the relation $\omega_1>\omega_2>\omega_3>\ldots>\omega_n$, and we can easily find

$$\begin{gathered}
2\omega_1 > \omega_1+\omega_2 > \omega_1+\omega_3 > \ldots > \omega_1+\omega_n \\
2\omega_2 > \omega_2+\omega_3 > \omega_2+\omega_4 > \ldots > \omega_2+\omega_n \\
\cdots \\
2\omega_{n-2} > \omega_{n-2}+\omega_{n-1} > \omega_{n-2}+\omega_n \\
2\omega_{n-1} > \omega_{n-1}+\omega_n > 2\omega_n
\end{gathered}$$

By selecting suitable pump wavelengths to satisfy $\omega_1+\omega_n>2\omega_2$, $\omega_2+\omega_n>2\omega_3$, $\cdots$, $\omega_{n-3}+\omega_n>2\omega_{n-2}$, $\omega_{n-2}+\omega_n>2\omega_{n-1}$, $\omega_{n-1}+\omega_n>2\omega_n$, relations listed above can be connected end to end, resulting into $2\omega_1>\omega_1+\omega_2\sim\omega_1+\omega_n>2\omega_2>\omega_2+\omega_3\sim\omega_2+\omega_n>2\omega_3>\cdots>2\omega_{n-2}>\omega_{n-2}+\omega_n>2\omega_{n-1}>2\omega_n$. It can be seen that sum-frequency signals are regularly divided by SH signals. The case that n equals to 3 is illustrated in Fig. 4(a).

Section 3: Derivation for the ratio of spectral bandwidths between second harmonic and superluminescent light-emitting diode pump.

The normalized Gaussian-shaped spectrum of superluminescent light-emitting diode (SLED) source can be assigned as $P_\omega(\lambda)=e^{-\omega x^2}$ (a>0), and its 10-dB bandwidth is

$$\mathrm{BW}_\omega = 2\lambda_0 = 2\sqrt{-\frac{1}{a}\ln P_\omega(\lambda_0)}\,, \tag{S1}$$

where $P_\omega(\lambda_0)$ is one tenth of the maximal power.

Assuming phase-matching condition is satisfied, the quadratic relation between pump and SH can be expressed as

$$P_{2\omega} \propto P_\omega^2 \,\mathrm{sinc}^2\left(\frac{\Delta\beta L}{2}\right) \approx P_\omega^2\,, \tag{S2}$$

therefore, the 10 dB bandwidth of SH spectrum can be obtained from $P_\omega^2(\lambda)=\mathrm{e}^{-2\omega\lambda^2}$, whose bandwidth can be express as $2\sqrt{-\frac{1}{2a}\ln P_\omega^2(\lambda_0')}$, where $P_\omega^2(\lambda_0')$ equals to $P_\omega(\lambda_0)$. However, due to the frequency-doubling process, bandwidth of SH spectrum equals to half that of $P_\omega^2(\lambda)$

$$\mathrm{BW}_{2\omega} = \sqrt{-\frac{1}{2a}\ln P_{\omega}^{2}\left(\lambda_0'\right)}\,. \tag{S3}$$

Thus, the ratio of spectral bandwidths between SH and pump is

$$\frac{\mathrm{BW}_{2\omega}}{\mathrm{BW}_{\omega}} = \frac{\sqrt{-\frac{1}{2a}\ln P_{\omega}^{2}\left(\lambda_0'\right)}}{2\sqrt{-\frac{1}{a}\ln P_{\omega}\left(\lambda_0\right)}} = \frac{1}{2\sqrt{2}} \approx 0.354\,, \tag{S4}$$

Section 4: Power dependence of third-harmonic generation under 1550 nm picosecond laser pump.

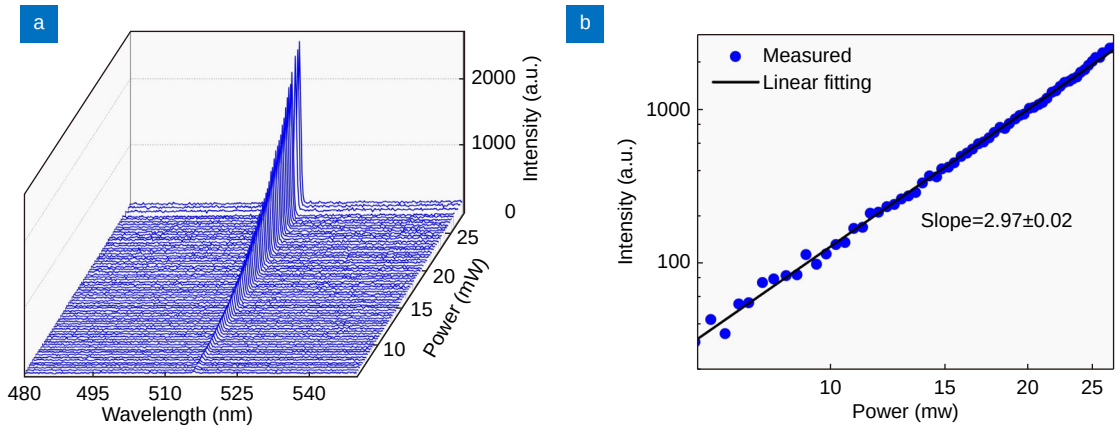

Fig. S2 | Spectral evolution of TH at 516.3 nm under the 1550 nm picosecond laser pump.

Section 5: Broadband second harmonic from the GaSe-transferred microfiber implemented by an amplified spontaneous emission source.

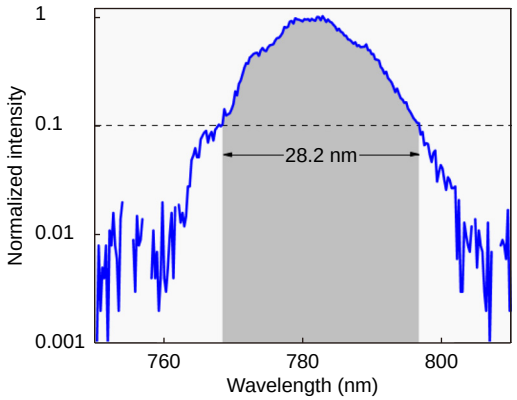

Fig. S3 | Broad SH spectrum excited by an amplified spontaneous emission source.

Section 6: The origination of the polarization dependent second harmonic and the equivalent coverage ratio.

The origination of the polarization dependent SH and the equivalent coverage ratio can be analyzed from:

$$\begin{bmatrix} P_x^{(2)}(2\omega) \\ P_y^{(2)}(2\omega) \\ P_z^{(2)}(2\omega) \end{bmatrix} = 2\varepsilon_0 \begin{bmatrix} 0 & 0 & 0 & 0 & 0 & -d_{22} \\ -d_{22} & d_{22} & 0 & 0 & 0 & 0 \\ 0 & 0 & 0 & 0 & 0 & 0 \end{bmatrix} \begin{bmatrix} E_x^2(\omega) \\ E_y^2(\omega) \\ E_z^2(\omega) \\ 2E_y(\omega)E_z(\omega) \\ 2E_x(\omega)E_z(\omega) \\ 2E_x(\omega)E_y(\omega) \end{bmatrix}, \tag{S5}$$

this equation describes the relationship between the second-order nonlinear polarization, the nonlinear tensor and elec-

tric field components of incident pump light. $\boldsymbol{E}(\omega)$, $\boldsymbol{P}(2\omega)$ represent electric field vectors of pump light and second-order nonlinear polarization (with x and y correspond to zigzag and armchair directions, respectively). d_{ij} represents nonzero element of ε-GaSe.

It can be written as:

$$\begin{bmatrix} P_x^{(2)}(2\omega) \\ P_y^{(2)}(2\omega) \\ P_z^{(2)}(2\omega) \end{bmatrix} = 2\varepsilon_0 \begin{bmatrix} -2d_{22}E_x(\omega)E_y(\omega) \\ -d_{22}E_x^2(\omega) + d_{22}E_y^2(\omega) \\ 0 \end{bmatrix} \propto \begin{bmatrix} -2E_x(\omega)E_y(\omega) \\ -E_x^2(\omega) + E_y^2(\omega) \\ 0 \end{bmatrix}, \tag{S6}$$

by combining its components, the vector form of the nonlinear polarization can be rewritten as

$$\boldsymbol{P}^{(2)}(2\omega) \propto -2E_x(\omega)E_y(\omega)\hat{\mathbf{x}} + [E_y^2(\omega) - E_x^2(\omega)]\hat{\mathbf{y}}\ , \tag{S7}$$

and the produced SH can be expressed as

$$I(2\omega) \propto \left|\boldsymbol{P}^{(2)}(2\omega)\right|^2 \propto [-2E_x(\omega)E_y(\omega)]^2 + [E_y^2(\omega) - E_x^2(\omega)]^2 = [E_x^2(\omega) + E_y^2(\omega)]^2\ . \tag{S8}$$

Substituting E_x=$E_t$cosθ, E_y=$E_t$sinθ ($\boldsymbol{E}_t$=$\boldsymbol{E}_x$+$\boldsymbol{E}_y$) into Eq. (S8), we can obtain that

$$I(2\omega) \propto E_t^4\ , \tag{S9}$$

it can be seen that SH intensity is proportional to the quartic function of projection of $\boldsymbol{E}(\omega)$ to the local x-y plane element of the GaSe coating. The projection changes regularly with the polarization direction of pump light, and the excited SH will change accordingly. According to the fundamental relationship in Eq. (S9), we calculated the polarization dependent SH in Fig. 1(g) and obtianed the equivalent coverage ratio.

Section 7: The calculation and calibration results of conversion efficiencies for references cited in Table 1.

To facilitate comparison, the conversion efficiencies presented in Table 1 have been unified in the same unit. Specifically, the normalized conversion efficiency on per unit length in the work in ref.[26] of the main text is directly given as 5×10^{-10} %W^{-1}cm^{-1}, which is equivalent to 5×10^{-11} %W^{-1}mm^{-1}. In ref.[14], the length of the silica photonic crystal fiber and average pump power are 150 mm and 500 mW, respectively. With the given absolute conversion efficiency of 1.6×10^{-6}, the normalized conversion efficiency per unit length is calculated as 2.1×10^{-6} %W^{-1}mm^{-1}. In ref.[31], the length of the doped fiber and average pump power are 25 mm and 370 mW. With the given absolute conversion efficiency of 10^{-8}, the normalized conversion efficiency per unit length is calculated as 1.1×10^{-7} %W^{-1}mm^{-1}. From Fig. 4 of ref.[32], the normalized conversion efficiency is approximately 2×10^{-4}W $^{-1}$. The nonlinear interaction length is 230 mm, and the normalized conversion efficiency per unit length is 8.7×10^{-5} %W^{-1}mm^{-1}. In ref.[3], the length of the hollow-core fiber is 250 mm, and the used pump power is at the level of 10^2 mW. Combined with the given absolute conversion efficiency of 10^{-4}, the normalized conversion efficiency per unit length is calculated as 4×10^{-4} %W^{-1}mm^{-1}. In ref.[29], SH is enhanced by 20 times compared with that excited in a pristine microfiber. Considering the 60 μm length of the transferred WS_2 coating, the normalized enhancement factor per unit length is calculated as 333 times·mm^{-1}.

In our previous work, the absolute power of SH has been challenging to measure directly with a power meter, and the conversion efficiencies were estimated through indirect measurement and calibration methods, which may have introduced errors. Fortunately, the proposed method in this work ensures a strong SH of nanowatt-level, allowing us to directly measure the collected SH by a power meter. This provides us a new method to calculate the weak SH power and corresponding conversion efficiencies. The main steps of this method can be summarized into three points: 1) Recording the SH absloute power/intensity count using a power meter/spectrometer under high/low pump power, respectively. 2) Calculating the conversion coefficient between unit power and one count. 3) Deriving the SH power and its conversion efficiency. By using the above method, we updated conversion efficiencies of the previous work (ref.[7, 24, 27, 28, 30]) for accuracy. Taking the losses in the experimental system into account, normalized conversion efficiencies of ref.[24] are updated to 1.6×10^{-5} %W^{-1}(4.0×10^{-6} %W^{-1}mm^{-1}) and 7.7×10^{-8} %W^{-1}(1.9×10^{-8} %W^{-1}mm^{-1}) under picosecond or continuous-wave (CW) pump. Similarly, the normalized conversion efficiency of ref.[27] is updated to 3.4×10^{-11} %W^{-1}(1.7×10^{-11} %W^{-1}mm^{-1}) under CW pump. The normalized conversion efficiency of ref.[30] is estimated to be 5.4×10^{-9} %W^{-1}(1.5×10^{-8} %W^{-1}mm^{-1}) under picosecond pump. The normalized conversion efficiency of ref.[28] is updated to 2.4×10^{-7}

$\%W^{-1}(4.2\times10^{-7}$ $\%W^{-1}mm^{-1})$ under picosecond pump. The normalized conversion efficiency of ref.[7] is updated to 1.7×10^{-6} $\%W^{-1}$ under picosecond pump. The normalized conversion efficiencies of this work are estimated to be 3.2×10^{-3} $\%W^{-1}(0.08$ $\%W^{-1}mm^{-1})$ and 1.3×10^{-7} $\%W^{-1}(3.2\times10^{-6}$ $\%W^{-1}mm^{-1})$ under picosecond or CW pump.